

Evaluation of Si nanowire as biosensing device

M. FLORESCU^{a*}, W. HU^b

^a*Faculty of Medicine, Transilvania University of Brasov, Str. N. Balcescu 56, 50019, Brasov, Romania*

^b*Electrical Engineering Department, University of Texas at Dallas, Richardson TX 75080, USA;*

Using devices, such biosensors, employing biomolecules as analytical tools offer advantages compared with conventional methods due to their simplicity, specificity, selectivity and quick response for real-time analysis. Si nanowire (SiNW) biosensors have recently emerged as a unique electronic biosensor platform for detecting biochemical species with ultrahigh sensitivity and rapid detection time. Despite of the great achievements in this field, the SiNW sensor reliability is seldom studied, which is however of vital importance for the technology to become practically relevant. The distribution of the protein molecules on biosensor surface is a function of the environmental variables, especially buffer used for sample preparation, as well as the interaction with other biomolecules. We report the effects of ion strength, liquid flow rate set by the pressure applied, and device biasing voltage on the response and stabilization times, drifting, sensitivity, and hysteresis of pH sensing of the Si nanowire bio-FETs. Using pH sensing as the model, we found some of these factors are correlated and must be controlled in order to obtain reliable sensing.

(Received April 9, 2015; accepted June 24, 2015)

Keywords: bio-FET, biosensors, SiNW, bioactivity

1. Introduction

There have been significant efforts in developing both optical and electronic type sensors to quantify biochemical markers at low abundance, which is critical to many disciplines in the life sciences, health care, disease diagnosis, drug discovery, environment monitoring and bioterrorism [1-8]. Compared to optical sensors, the advantages are of electronic sensor in small size, low manufacturing cost, label-free real-time detection, multiplexing options [9-11]. The field-effect transistor (FET) biosensor is a type of electronic device that promises to advance point-of-care testing of real samples such as blood for health care, beverages for food industry or water samples for environmental applications by offering desirable characteristics such as portability, high sensitivity, high specificity, low sample volume, brief detection time and low power consumption [12-14]. Ion sensitive FET (ISFET) are natural candidates for electrically based sensing of charged analytes due to the dependence of channel conductance on both gate voltage and surface charges resulting from the binding of (bio)molecules to the channel surface coated with probes or receptors. Shrinking the channel volume (width, length, and thickness) of the FETs will increase its sensitivity. In one extreme case, using a CVD nanowire (NW) as sensing element, NWFETs have shown supreme sensitivity for detection of protein, DNA, virus, and cells in solution [15, 16]. Despite great scientific achievements made recently, electronic sensors using these nanostructures still exhibit lack of repeatability and reliability. Some issues are for example the temporal stability, device drift issues or effect of back-gate biasing [17-19]. Many parameters are of extreme importance when designing a device to perform molecular analysis of biological samples where the molecular analyte concentration is low: high sensitivity,

highly specific molecular analyte sensing, short detection time, etc. [20]. The pH of the buffer used for sample solutions preparation has an important role in sensing, especially in the biosensing and usually not adequately taken into account. Previously, it was reported that a change of the transistor conductance according to the pH of the solution is observed on a large pH interval, even for small variations of 0.1 pH units and physico-chemical parameters such as gate voltage and buffer salinity can affect the sensitivity of the measurements [21]. The total electrolyte concentration is also affecting important properties of the solutions; thus ionic strength of the used solutions became important in biosensing using NWFETs by affecting Debye length (the distance at which a unit charge is reduced to $1/e \approx 0.37$, meaning that the protein charges are screened by 63%). A way to increase the performance of NWFET sensors is to dilute the sensing buffer drastically, but Lloret et al. showed that this can have an important effect on the function of the proteins: it significantly affects the pH stability of the sensing buffer, which consequently impacts the charge of the protein and thus the response and signal-to-noise ratio in the sensing experiments [22].

In this study, we have investigated the effects of supporting buffer usually used for preparation of biological sample solutions (pH, ion strength and liquid flow rate set by the pressure applied of the buffer solutions) together with device biasing voltage on the response and stabilization times, drifting, sensitivity, hysteresis of pH sensing on NWFETs sensor response. These parameters are correlated and must be controlled in order to obtain reliable future biosensing.

2. Material and methods

2.1. Device Fabrication

NWFET devices were fabricated using lithographic processes on Silicon on Insulator wafer (SOI) and use multi-NWs or nanograting (NG) as sensing element instead of conventional single nanowire to avoid discrete dopant fluctuation and achieve high device uniformity [23] Details of fabrication is reported elsewhere [24] Photolithography and Cl_2 plasma etching were applied to define active device area and source drain contact pads. Ion implantation with phosphorous (10^{19} cm^{-3}) was used to form source drain junctions for NMOS. Then, e-beam lithography and Cl_2 plasma etching was used to define the Si NG structures measured as $\sim 50 \text{ nm}$ in width, 30 nm in height, $20 \mu\text{m}$ in length. A 3 nm SiO_2 layer was thermally grown around the NG as gate dielectrics. The area other than the NG was passivated by silicon nitride. Figure 1 shows the schematic and an SEM image of a fabricated NG-FET device.

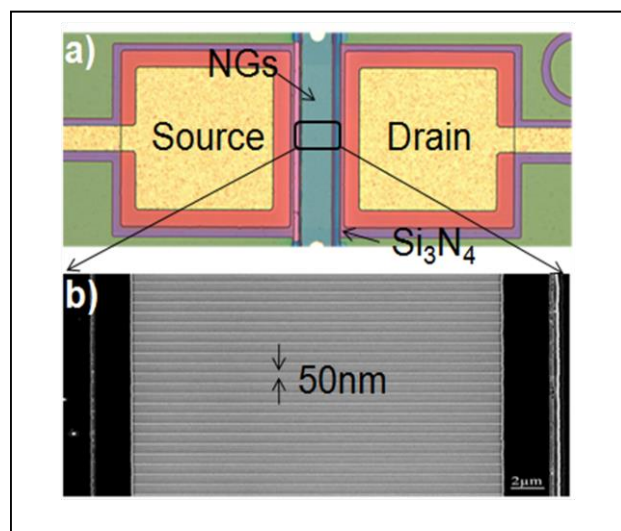


Fig. 1. a) Schematic of Si nanograting FETs (100 NWs).
b) SEM image of the Si nanograting

NG-FET devices with 100 NWs connecting source and drain have shown uniform and good performance with ON/OFF $\sim 10^6$, SS of $\sim 60 \text{ mV/dec}$, and V_t of $\sim 1 \text{ V}$. The gate leakage currents are low (pico amps). Before measurements the surface of NG-FET was piranha treated for 2 mins. The devices were then packaged with a polydimethylsiloxane (PDMS) piece containing a sealed micro-machined fluidic channel [25]. A metal wire (Ag/AgCl) was inserted through the PDMS into the solution serving as the solution gate.

2.2. Device Measurements

The NG-FETs chip sealed into mechanical clamps was fixed into the probe station and connected to a Keithley 4200S analyzer. Typical current-voltage (I-V) characteristics of n-type NG-FETs (drain current I_d as a

function of reference gate voltage V_g at a drain voltage V_d of 100 mV plotted in a logarithmic scale - data not shown) and current-time (I_d -t) plots (Fig. 2) were recorded. A reference electrode Ag/AgCl wire was used as solution gate to bias NGFETs in the solution. Two voltages biasing were chosen: one in the sub-threshold region (0.45 V) and one in the linear region (1.4 V).

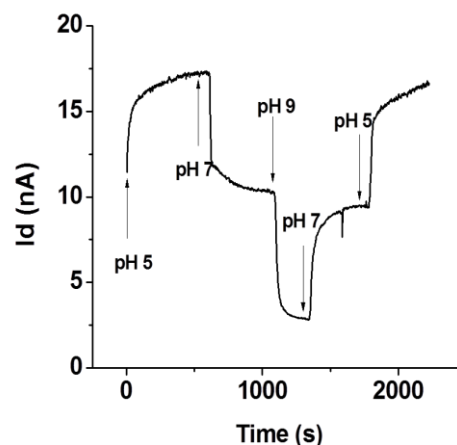


Fig. 2. Representative current-time (I_d -t) plot.
Experimental conditions for this particular plot:
KPB buffer, 10 mM , $p = 5.0 \text{ PSI}$, $U_g = 0.45 \text{ V}$

The buffer solutions usually used for biological sample preparation and dilution was circulated through micro-machined fluidic channel and flowing rate was set by the pressure applied (1.5 , 3.0 and 5.0 PSI) using a pump. Tubing used for microfluidic channel connection with liquids reservoirs were PEEK type with 0.25 mm inner diameter. The buffer used for all the experiments was potassium phosphate buffer (KPB) which consists of a mixture of monopotassium dihydrogen phosphate and dipotassium monohydrogen phosphate with deionized water in various ratios. Three ions concentrations were used (100 mM , 10 mM and 1 mM) with three pH values (5 , 7 and 9). Using a manually switch for each concentration the buffer solutions pH was sweep from $5 \rightarrow 7 \rightarrow 9$ (forward sweep) and then sweep back (backward sweep).

3. Results and discussions

Achieving device stability and high performance in buffer solutions is vitally important for using NG-FETs in biosensing. The high salt concentration in solution poses a challenge for device stability since mobile ion contamination is known as a constant threat to semiconductor device performance and reliability. The pH of the buffer solutions has an important role in sensing, especially in the biosensing. The distribution of the protein molecules among different conformational states depends on Gibbs free energy of each state, which in turn is a function of the environmental variables (pH, ionic strength, temperature), as well as the interaction with other

biomolecules [26]. Thus for developing high performance biosensors it is important to first know and understand how environmental variables influence the performance of the NGFETs. Thereby the I_d - t plots in all experimental conditions were analyzed aiming the stabilization of the signal in terms of presence or absence of device drift and the sensitivity device with response to pH, the hysteresis together with response and stabilization times of the sensor to be determined as ionic strength, flow rate set by the pressure applied and pH of buffer solutions are swept.

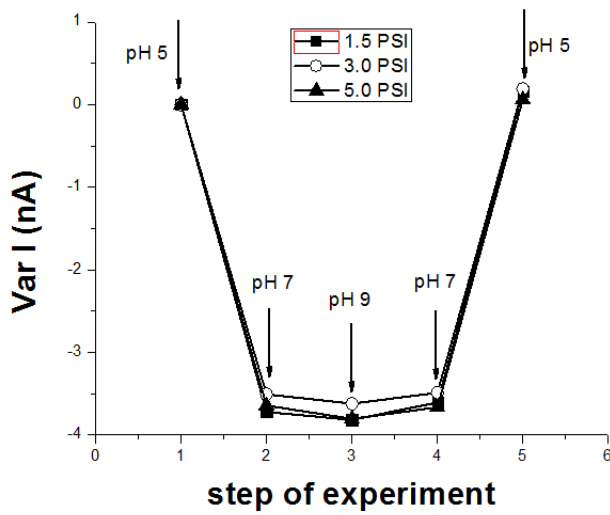


Fig. 3. I_d (nA) vs. pH sweeping from 5 \rightarrow 7 \rightarrow 9 \rightarrow 7 \rightarrow 5, 100 mM K-PBS, $V_g = 0.45$ V at different applied pressures.

3.1 Voltage biasing

Analyzing the device response we observed that for a voltage biasing in the sub-threshold region (0.45 V) the signal doesn't show any drift and the stabilization of the signal depends just on flow rate set by the pressure applied. For all pressures applied the sensor sensitivity is similar as pH electrolyte changes; for both pH 5 and 7 a slightly different behavior for 10 mM was observed. Figure 3 shows the results for 100 mM concentration of KPB when pH is swept 5-7-9-7-5 for the three applied pressures.

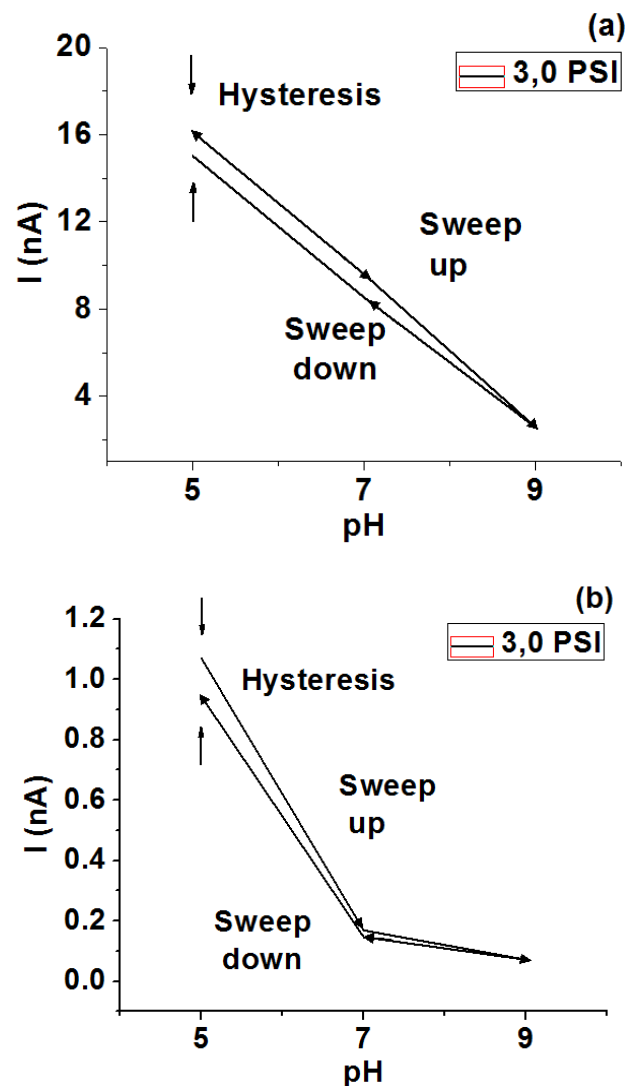


Fig. 4. I_d (nA) vs. pH sweeping from 5 \rightarrow 7 \rightarrow 9 \rightarrow 7 \rightarrow 5 at 3 PSI (flow rate) and $V_g = 0.45$ V for (a) 10 mM K-PBS; (b) 1 mM K-PBS.

Fig. 4 shows the response of the NG-FETs for pH sweeping at the same pressure applied of 3.0 PSI for salt concentrations of 10 mM and 1 mM.

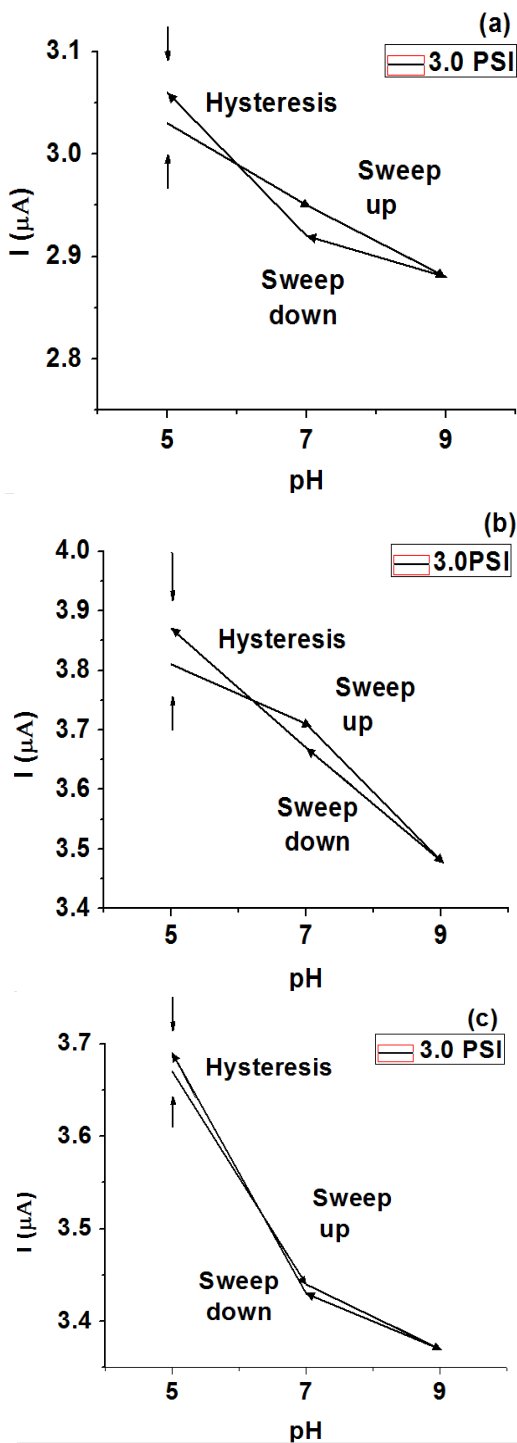


Fig. 5. I_d (μA) vs. pH sweeping from 5 \rightarrow 7 \rightarrow 9 \rightarrow 7 \rightarrow 5 at 3PSI and $V_g = 1,4$ V for (a) 100 mM, (b) 10mM, and (c) 1mM K-PBS.

When a voltage biasing in the linear region (1.4 V) was set, for all three salt concentrations the signal doesn't present any drift; stabilization of the signal depends just on pressure applied and the hysteresis was present for both pH 5 and 7. Figures 5 shows the variation of current when pH was swept 5-7-9-7-9 for all concentrations at pressure applied of 3PSI. The hysteresis was present for both pH 5 and 7 and the sensor sensitivity is similar as pH electrolyte

changes, a little higher for 1.5 PSI. Stabilization process is similar for pH changes for all three pressures applied; the few differences are due to particular behavior of the chip for an electrolyte concentration of 100 mM. The drift for 1 mM was not present when pressures of 1.5 and 5 PSI were applied, stabilization of the signal depending just by pressure applied, while for a pressure of 3 PSI the drift was present, especially when pH changes between 5 \leftrightarrow 7. The sensor sensitivity is similar for flow rates established by pressures of 1.5 and 5.0 PSI, while for a pressure of 3.0 PSI the sensitivity was different at pH 5. Stabilization of the signal seems also to be slightly dependent on the pressure applied.

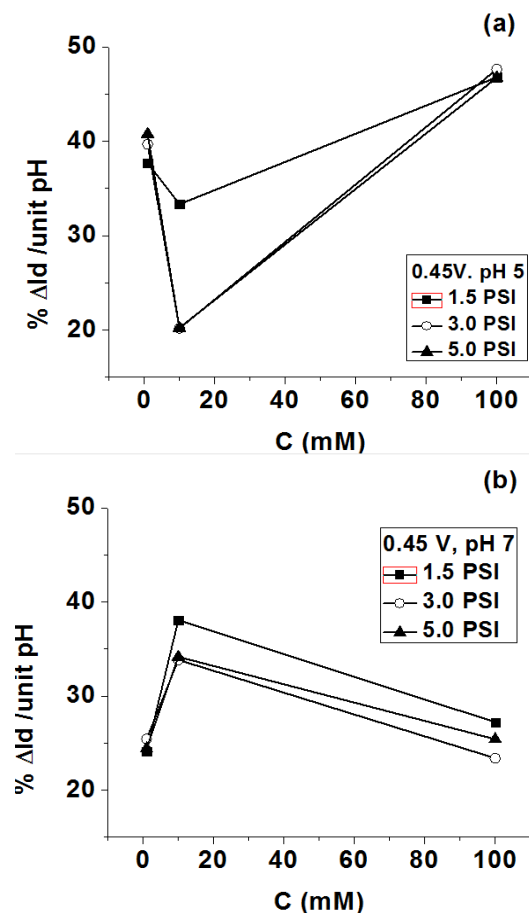


Fig. 6. Variation of sensitivity for (a) pH sweep 5 \leftrightarrow 7 and (b) pH sweep 7 \leftrightarrow 9, vs. salt concentration. $V_g = 0.45$ V

3.2 Effects on Sensitivity and Hysteresis

The sensitivity of device with response to pH is defined as % of drain current I_d change per unit pH. In low biasing voltage (0.45V) for 100 mM and 1 mM of salt concentrations at all pressure applied the sensitivity of NGFETs is higher when pH is swept between 5 \leftrightarrow 7 (Table 1). This is not happening when concentration of 10 mM is flowed on the chip surface and the device had higher sensitivities for fluid environment changing between neutral and basic pH. Low biasing voltage was not causing

device response sensitive to pressure applied for a constant salt concentration, exception for an electrolyte concentration of 10 mM at 1.5 PSI (Figure 6). The highest average sensitivity was obtained for 100mM, followed by the one obtained for 1 mM (for 5 ↔ 7 pH swept) and for 10 mM when pH was swept between 7 ↔ 9 (Table 1).

Table 1. Variation of device sensitivity versus salt concentrations for low biasing voltage.

pH sweep	Low Gate Voltage (V)			
	C (mM)	Pressure (PSI)	Baseline current (nA)	Sensitivity (% of ΔI_d / pH)
5↔7 7↔9	100	1.5	4.00	46.78
			0.28	27.23
5↔7 7↔9		3.0	3.77	47.63
			0.27	23.40
5↔7 7↔9		5.0	3.94	46.73
			0.30	25.42
5↔7 7↔9	10	1.5	4.29	33.33
			1.76	38.07
5↔7 7↔9		3.0	16.11	20.19
			9.59	33.84
5↔7 7↔9		5.0	17.21	20.24
			10.25	34.17
5↔7 7↔9	1	1.5	0.97	37.69
			0.14	24.13
5↔7 7↔9		3.0	1.07	39.67
			0.17	25.44
5↔7 7↔9		5.0	1.10	40.77
			0.17	24.43

Table 2. Variation of device sensitivity versus salt concentrations for high biasing voltage.

pH sweep	High Gate Voltage (V)			
	C (mM)	Pressure (PSI)	Baseline current (μ A)	Sensitivity (% of ΔI_d / pH)
5↔7 7↔9	100	1.5	3.02	2.65
			2.88	1.65
5↔7 7↔9		3.0	3.03	1.82
			2.95	0.93
5↔7 7↔9		5.0	3.08	1.70
			2.98	1.17
5↔7 7↔9	10	1.5	3.84	2.17
			3.72	2.96
5↔7 7↔9		3.0	3.81	1.97
			3.71	2.83
5↔7 7↔9		5.0	3.92	1.85
			3.79	2.11
5↔7 7↔9	1	1.5	2.79	1.97
			2.69	0.28
5↔7 7↔9		3.0	3.67	3.34
			3.44	0.94
5↔7 7↔9		5.0	2.85	1.93
			2.74	0.64

The conventional hysteresis of MOSFET is defined as gate voltage shifts depending on subthreshold slope and drain current for forward (I_{fs}) and for backforward (I_{bs}) sweep. $\Delta I/I$ is monotonic correlates to this hysteresis. So it is simple for us to just use $\Delta I/I = (I_{fs} - I_{bs})/I_{fs}$ as hysteresis, in other words, the variation of sensitivity between forward and backward sweeping can be treated as sensing hysteresis. The hysteresis at low biasing voltage seems to be dependent on salt concentrations for both pH variations (data not shown).

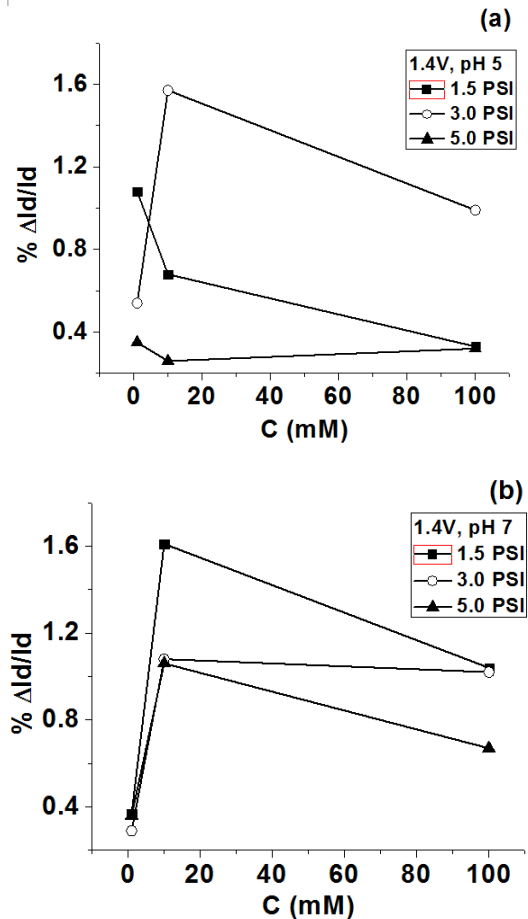


Fig. 7. Variation of hysteresis (a) for pH sweep 5 ↔ 7 and (b) for pH sweep 7 ↔ 9, vs. salt concentration. $V_g = 1.4$ V.

In the case of pH sweeping 5 ↔ 7 higher salt concentrations reduces the hysteresis. For both pHs sweeping the higher pressure reduces the device hysteresis with an exception for 1 mM for 7 ↔ 9 pH change when the hysteresis has similar values. For majority of the measurements at high voltage biasing the sensitivity of NG-FETs is slightly higher when pH is swept between 5 ↔ 7 (Table 2) when salt concentration doesn't affect the sensitivity of device to flow rate, except one case at 3.0 PSI for 1 mM when the average sensitivity was higher than other cases. Exception appears for 10 mM concentration in 7 ↔ 9 pH range when it shows highest sensitivity for all pressures applied (average of 2.63 % ΔI_d /unit pH compared with of 1.25 % ΔI_d /unit pH for 100 mM and 0.62 % ΔI_d /unit pH for 1 mM). The sensing hysteresis also

appears when high biasing is used for all salt concentrations at both pH 5 and 7; it has very small values and seems generally to be independent with salt concentration and flow rate variation for 5↔7 pH sweep (Figure 7). For 7↔9 pH sweep, higher salt concentrations increase the hysteresis, especially for 10 mM salt concentration. For both pH ranges the pressure applied seems to don't influence the hysteresis for a constant salt concentration.

3.3 Effects on Response Time

A low response time of the device, t_r , is desired. Response of the NG-FETs seems to depend strongly on the pressure applied and in small extent on salt concentrations. For all salt concentrations t_r generally decreased (around 50%) when higher values of pressure were applied, for both low and high biasing voltages (see Figure 8). It can be observed that generally for 1 mM and 10 mM t_r is longer, especially for high biasing voltage. When 100 mM was used the response of the device was generally fast, and slightly faster for higher biasing voltage. This situation was present for 1.5 PSI and 3.0 PSI and not for 5.0 PSI when the t_r has the similar value in both biasing voltages for all electrolyte concentrations (around 30 s).

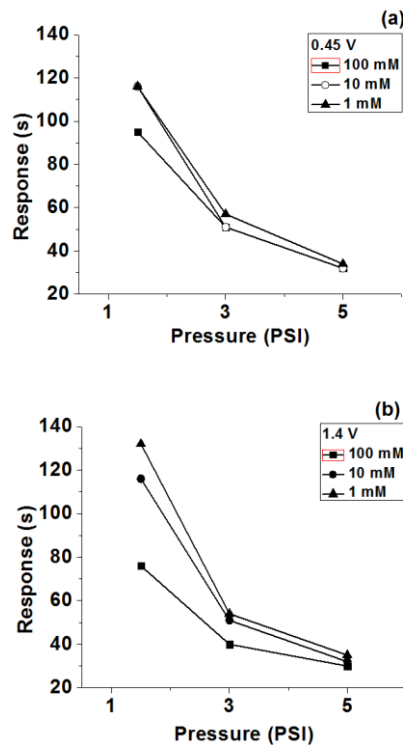


Fig. 8. Averaged response time for (a) $U_g=0.45$ V and (b) $U_g=1.4$ V, vs. pressure under various salt concentrations.

3.4 Effects on Stability

The chip with NG-FETs was kept in water when not in use. This fact can both help keeping the electric charges mobility from the surface of the sensing surface (nanowires) and improving of the diffusion phenomena

through the interface at NG-FETs during measurements. Thus dehydration is avoided allowing for quick establishment of double layer to avoid long time drifting. General absence of the drift can also be attributed to keeping the chip surface in liquid (hydrated). Stabilization of the signal seems to depend on the pressure applied (flow rate) and ions concentrations. For salt concentrations of 100 mM and 10 mM the stabilization time generally decreased when higher values of pressure were applied for both low and high biasing voltages (see Fig. 9). It can be observed that for these two ions concentrations the stabilization of the electric signal occurs in a longer time (over 500 s) when higher biasing voltage was applied. When 1 mM was used the stabilization of the signal seems to be independently on the pressure applied and the stabilization time remains almost constant around 200 s (little smaller for 1.5 PSI and 5.0 PSI) for both low and higher biasing voltages.

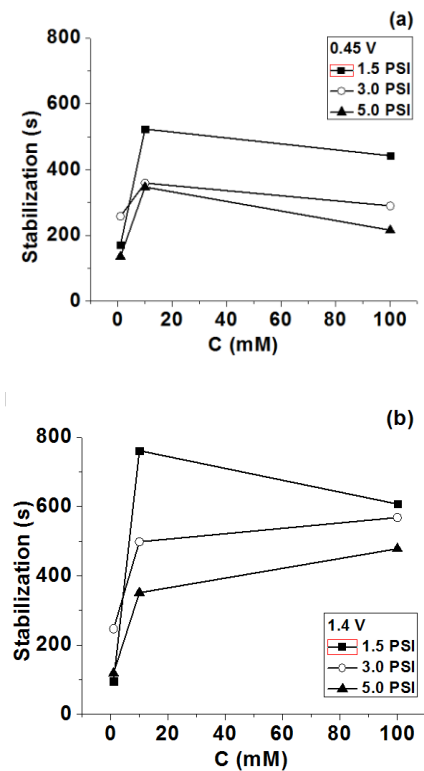


Fig. 9. Averaged stabilization time for (a) $U_g=0.45$ V and (b) $U_g=1.4$ V, vs. salt concentrations.

4. Conclusions

The phenomena at the surface of sensor (chip), when the electrolyte has flowed, have depended on the electrolyte concentrations, on flow rate set by the pressure applied and on the biasing voltage. Low biasing voltage (subthreshold) didn't determine a sensitive response of the device to pressure applied for a constant salt concentration, but the salt concentration has affected the sensitivity of the device. The highest average sensitivity (46.78% ΔI_d /unit pH) was obtained for 100mM, when pH was swept 5↔7. For high

biasing voltage (1.4V) the sensitivity of NG-FETs was sensitive to pH swept, but not at concentration of the electrolyte or pressure applied. It appears that the hysteresis is present in pH sensing both for pH 5 and 7 at both lower and higher biasing voltages. In high voltage biasing both the sensitivity and hysteresis present much smaller values compared with ones for sub-threshold voltage which is in correlation with literature. Hysteresis in this voltage generally seems to be independent with salt concentration and flow rate variation for pH sweep 5 \leftrightarrow 7, while for 7 \leftrightarrow 9 pH sweep the higher salt concentrations increase the hysteresis. At low biasing voltage for pH 5 the higher salt concentrations reduces the hysteresis and for both pHs higher pressure seems to reduce it.

Response of the NG-FETs seems to depend strongly on the pressure applied (flow rate) and in small extent on ions concentrations. For all three salt concentrations, the response time decreased when higher values of pressure were applied until 30 s for 5.0 PSI in both low and high biasing voltages. Stabilization of the signal seems to depend on the pressure applied (flow rate) and ions concentrations. General absence of the drift can be attributed to keeping the chip in liquid (hydrated) fact which allows quick establishment of double layer.

We may conclude that the lower biasing voltage will cause huge amount of charges and counter-ions to accumulate at the gate dielectric surfaces causing overcharging effect. The changes of electrolyte salt concentrations would make large interrupts to the double layer formation, causing shifts of device baseline and sensitivity to pH, facts not present at higher biasing voltage.

Acknowledgments

This work is partially supported by National Science Foundation (ECCS-0955027, CBET #1064574, IIP # 1127761), Texas Medical Consortium. Monica Florescu would acknowledge the funding of Transilvania University of Brasov Grant for her visiting professorship at UT Dallas to perform the work. The authors would like to thank Pengyuan Zang, Krutarth Trivedi, and Edward Castellana, Howard Tigelaar for setting up microfluidic system and useful discussions.

References

- [1] M. R. Kierny, T. D. Cunningham, B. K. Kay, *Nano Reviews* **3**, 17240 (2012).
- [2] A. L. Carvalho, I. N. Nishimoto, J. A. Califano, L. P. Kowalski, *Int. J. Cancer* **114**, 806 (2005).
- [3] Stat bite: worldwide cervical and uterine cancer incidence and mortality, 2002, *J Natl Cancer Inst.* **98**, 1031 (2006).
- [4] H. Kawaguchi, A. K. El-Naggar, V. Papadimitrakopoulou, H. Ren, Y. H. Fan, L. Feng, J. J. Lee, E. Kim, W. K. Hong, S. M. Lippman, L. Mao, *Podoplanin: J Clin Oncol*, **26**, 354 (2008).
- [5] W. J. Peveler, R. Binions, S. M. V. Hailes, I. P. Parkin, *J. Mater. Chem. A*, **1**, 2613 (2013).
- [6] E. Scallan, *Clin. Infect. Dis.* **44**, 718 (2007).
- [7] A.El-Ansary, L. M Faddah, *Nanotechnology, Science and Applications* **3**, 65 (2010).
- [8] P. S. Mead, L. Slutsker, V. Dietz, L. F. McCaig, J. S. Bresee, C. Shapiro, and e. al., *Emerg Infect Dis.* **5**, 607 (1999).
- [9] P. Bergveld, *Sensors And Actuators B* **88**, 1 (2003).
- [10] O. Lazcka, F. J. Del Campo, F. X. Munoz, *Biosensors & Bioelectronics*, **22**, 1205 (2007).
- [11] J. S. Daniels, N. Pourmand, *Electroanalysis* **19**, 1239 (2007).
- [12] J. H. Chua, Ru-Ern Chee, A. Agarwal, S. M. Wong, G.-J. Zhang, *Anal. Chem.* **81**, 6266 (2009).
- [13] E. Stern, A. Vacic, M. A. Reed, *IEEE Trans. Electron Devices* **55**, 3119 (2008).
- [14] L. de Smet, D. Ullien, M. Mescher, E. J.R. Sudhölter, *Organic Surface Modification of Silicon Nanowire-Based Sensor*, in: A. Hashim (Ed.), *Devices Nanowires - Implementations and Applications*, InTech, Available from: <http://www.intechopen.com/books/>.
- [15] Y. Cui, Q. Q. Wei, H. K. Park, C. M. Lieber, *Science*, **293** 1289, (2001).
- [16] E. Stern, J. F. Klemic, D. A. Routenberg, P. N. Wyrembak, D. B. Turner-Evans, A. D. Hamilton, D. A. LaVan, T. M. Fahmy, M. A. Reed, *Nature*, **445**, 519 (2007).
- [17] P. R. Nair, M. A. Alam, *IEEE Trans. Electron Devices*, **54**, 3400 (2007).
- [18] M. Asen Asenov, A. R. Brown, J. H. Davies, S. Kaya, G. Slavcheva, *IEEE Trans. Electron Devices*, **50**, 1837 (2003).
- [19] P. G. Fernandes, R.A.Chapman, O.Seitz, H.J.Stiegler, H.-C.Wen, Y.J.Chabal,and E.M.Vogel, *IEEE ELECTRON DEVICE LETTERS.* **33**, 447 (2012).
- [20] M. S. Makowski, A. Ivanisevic, *small* **7** 1863, (2011).
- [21] G. Lehoucq, P. Bondavalli, S. Xavier, P. Legagneux, P. Abbyad, C. N. Baroud, D. Pribat, *Sensors and Actuators B* 171– **172**, 127 (2012).
- [22] N. Lloret, R. S Frederiksen, T. C Møller, N. I Rieben, S.Upadhyay, L. De Vico, J. H Jensen, J. Nygard and K. L Martinez, *Nanotechnology* **24**, 035501 (2013).
- [23] D. Vasileska, W. J. Gross, D. K. Ferry, *Proceedings of the 1998 Sixth International Workshop on Computational Electronics*, 1998, p. 259.
- [24] R. Tian, S. Regonda, J. Gao, Y. Liu, Walter Hu, *Lab Chip* **11**, 1952 (2011).
- [25] T. Mizuno, J.-i. Okamura, A. Toriumi, *IEEE Trans. Electron Devices*, **41**, 2216 (1994).
- [26] N. Cremades, M. Bueno, J.L. Neira, A. Velázquez-Campoy and J.Sancho, *J Biol Chem.* **283**, 2883 (2008).

*Corresponding author: florescum@unitbv.ro